Chalcogenide Letters Vol. 17, No. 9, September 2020, p. 429 - 437

FABRICATION AND CHARACTERIZATION OF DYE-SENSITIZED SOLAR CELLS BASED ON MUREXID DYE AND INORGANIC CdS:Mn THIN FILMS

N. BALPINAR[a], F, GÖDE[b,*]
[a]*Department of Biology, Faculty of Arts and Science, Burdur Mehmet Akif Ersoy University, 15030 Burdur, Turkey*
[b]*Department of Physics, Faculty of Arts and Science, Burdur Mehmet Akif Ersoy University, 15030 Burdur, Turkey*

In this study, dye-sensitized solar cells (DSSCs) were designed utilizing Murexid dye as an absorbing material and manganese doped cadmium sulfide (CdS:Mn) thin films as transparent layers. The CdS:Mn thin films were synthesized on tin doped indium oxide coated glass substrates (ITO) at 90 ºC using chemical bath deposition method (CBD). The Mn-doping process was carried out at concentrations of 0%, 2%, 4% and 6% (in molar ratio of manganese ions to cadmium ions). The structural, morphological and optical properties of the CdS:Mn thin films were examined using x-ray diffractometer (XRD), atomic force microscope (AFM) and UV–visible absorption spectrometer. The effect of the nanoparticle size on the cell performance of DSSC was investigated by J-V curves. The results regarding electrical measurements indicated that the maximum efficiency of 3.40%. Our experimental results suggested that this heterojunction can be a good candidate for DSSCs.

(Received May 28, 2020; Accepted September 2, 2020)

Keywords: Chemical bath deposition, Mn-doped CdS thin films, Optical properties, Electrical properties, Dye sensitized solar cells

1. Introduction

The need for usage of renewable energy sources rapidly increases day by day even though fossil fuels are still the world's primary energy source. Solar energy is a kind of green energy that is sustainable. Green energy is a very important topic for all countries in that high levels of carbon dioxide in the atmosphere drive global climatic changes. Solar cells can be separated into three groups according to their developmental stages: the first-generation (crystalline silicon, gallium arsenic solar cells), second-generation (inorganic thin films: CuInSe2, CdTe, CdS/PbS, a-Si solar cells), and third-generation (dye sensitive solar cells, organic solar cells) [1-6]. Among them, the DSSCs are third-generation photovoltaic cells that convert sun light into electrical energy via folovoltaic event. Recent investigations show that rapid production at low cost for DSSC devices is quite possible. The fabrication of dye-sensitized solar cells (DSSCs) using semiconductor with die molecules have attracted a great deal of attention which is first examined by Gerischer et al. [7] and Tsubomura et al. [8] where they report several dyes as photo sensitizers and zinc oxide (ZnO) as a semiconductor.

In some studies, it is indicated that the efficiency of DSSCs can be reached to 11-12% using chemical synthetic dyes [9,10]. The dye plays a crucial role in designing efficient DSSCs since it harvests the light from the attached a wide band gap semiconductor surface leading to an increment in the absorption [11]. Khan et al. [12] fabricated DSSCs utilizing ZnO thin films which are prepared by a sol-gel spin coating process and reach energy conversion effeciency of 2.29%. Baxter et al. [13] designed DSSCs using ZnO nanowires as the photo-electrode and obtained power conversion efficiencies of 0.3%. The ZnO thin films used in DSSCs are doped with different metals such as Li [14], Cu [15], Al [16] and strontium [17 widely in the literature. However, there is no enough information concerning Murexid dye and Mn doped CdS thin films used in DSSCs.

* Corresponding author: ftmgode@gmail.com

In her previous work, Göde et al. [1] reach quantum efficiency of semiconductor thin film solar cells (Ag/ITO/CdS/PbS/Ag) up to 4.85%. This study aims at increasing photovoltaic performance of DSSCs using Murexid as dye sensitizer and inorganic CdS:Mn thin films. Note that Murexid dye and CdS:Mn thin films are utilized in designing DSSCs for the first time in this work.

2. Experimental details

2.1. Synthesis of CdS:Mn thin films

The CdS thin film was deposited by using chemical bath deposition method (CBD) in previous report [1]. In this study, CdS:Mn thin films were synthesized onto tin doped indium oxide coated glass substrates (ITO) with the sheet resistance of ≤ 10 Ω / sq and dimensions of 76 mm × 26 mm × 1 mm using CBD method. Before deposition, the ITO substrates were firstly cleaned by detergent, boiled in ultrapure water (18.2 M Ω cm) and then washed in methanol, acetone and ultrapure water for 10 min sequentially. In order to deposition of the CdS thin films, 30 ml of 0.1 M cadmium nitrate (CdN_2O_6 $4H_2O$), 12 ml of 1 M tri-sodium citrate ($C_6H_5Na_3O_7$ $5.5H_2O$), 30 ml 9.96 M ammonium hydroxide (NH_4OH) with the 25% purity and 10 ml of 1 M thiourea (NH_2CSNH_2) were used. Then, to get 100 ml solution, the rest was completed by adding ultrapure water. As a dopant source, 0.1 M manganese acetate [$Mn(CH_3COO)_2$] was used. The doping concentration of Mn ions in the solution was adjusted as 0%, 2%, 4% and 6% (in molar ratio of manganese ions to cadmium ions). All of the films were obtained at 90 ºC waited for 2 h.

2.2. Preparation of DSSCs

Dye solution was prepared by adding 0.5 g of Murexid powder [($C_8H_8N_6O_6$); Ammoniumpurpurat metal indicator ACS; MA = 284.19 g/mol; Riedel-de Haën, Germany)] in~~to~~ 10 ml of ethanol. The solution was stirred using magnetic stirrer and left at room temperature for one day in order to achieve the desired viscosity. In the fabrication process of the DSSCs, the CdS:Mn thin films were deposited on ITO substrates using CBD technique, and dye was dropped onto the~~se~~ films. In the DSSCs, inorganic CdS:Mn thin films were used as transparent layers which accepts electrons from the photoexcited dye/sensitizer. In order to make a contact from dye, another ITO substrate with Ag contact was attached to the dye by forceps. The contacts on the films were made using silver paste. The structure of the fabricated DSSC was indicated in Fig. 1(a), and the molecular formula of Murexid was shown in Fig 1(b).

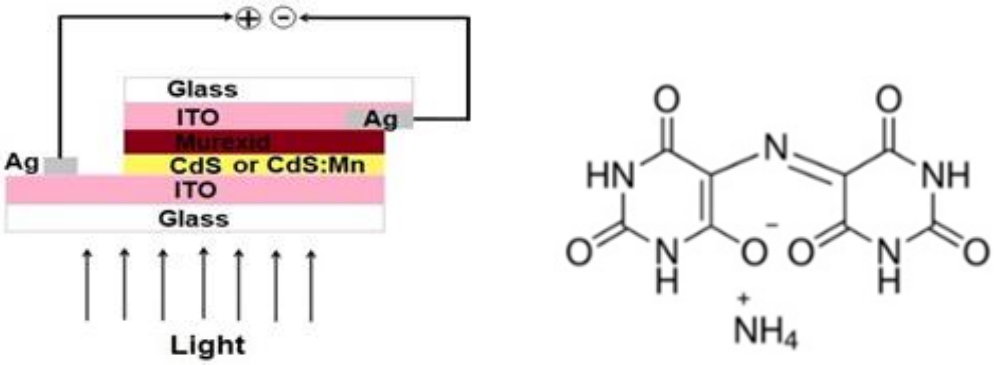

Fig. 1. Schematic diagram of the DSSCs and molecular formula of Murexid.

2.3. Characterization

Structural characterization of the CdS:Mn thin films were carried out using a x-ray diffractometer (XRD) (Bruker A8 Advanced) with Cu Kα (0.154 nm) radiation over a range of 2θ angle from 20° to 70°. The surface morphology of the films was investigated using a park system XEI Atomic Force Microscope (AFM) in non-contact mode. The UV–vis spectrophotometer (PG-

T60) was used to measure absorption and transmittance spectra of the films in the visible range of the solar spectrum. The electrical characteristics of the DSSCs were performed by a Keithley 2400 current-voltage source measuring system and obtained after lightening at 7w led lamp.

3. Results and discussion

3.1. Structural properties of CdS:Mn thin films

XRD patterns of the present films grown on ITO substrates at different Mn doping concentrations were indicated in Fig. 2. The reflection peaks were observed approximately at 2θ = 25.28º, 26.64º, 44.17º and 52.14º correspond to the (100), (002), (110) and (112) crystallographic planes and the peaks coincide with those of hexagonal wurtzite crystal structure according to JCPDS card No. 41-1049. It was observed that the films had polycrystalline structure, were showed diffraction peaks belonging to ITO substrates and were exhibited no extra phases involving Mn compounds. Moreover, the intensity of peak considering (002) plane decreased as a result of addition Mn into CdS film. As seen in Fig. 2, the crystallinity of the CdS film was deteriorated with increasing Mn dopant. This could be due to the formation of stresses by the difference in ion size between cadmium and the dopant material and the segregation of dopant in grain boundaries for high doping concentrations. Observed structural parameters were compared with standard values in Table 1.

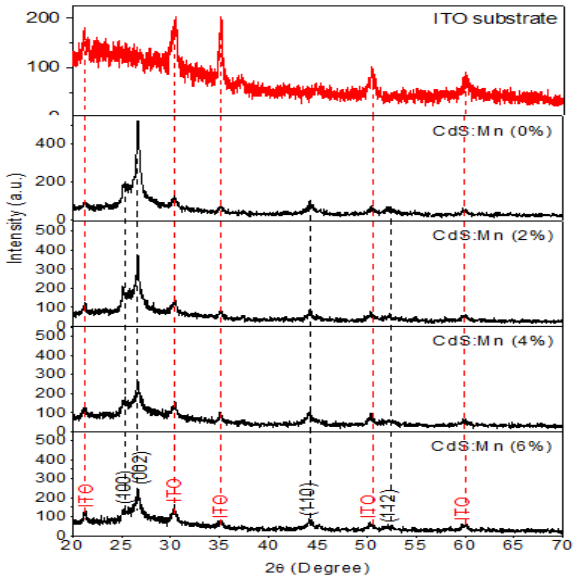

Fig. 2. X-ray diffraction pattern of CdS:Mn thin films.

Table 1. Structural parameters of the CdS thin films with different Mn concentration.

Material	Observed values		Standard values		D (nm) (002)	a (Å)	c (Å)	(hkl)
	2θ(°)	d (Å)	2θ(°)	d (Å)				
CdS	25.28	3.519	24.81	3.586	138	4.06	6.69	(100)
	26.64	3.344	26.51	3.360				(002)
	44.17	2.049	43.68	2.071				(110)
	52.14	1.753	52.80	1.733				(112)
CdS:Mn 2%	25.19	3.531	24.81	3.586	119	4.08	6.69	(100)
	26.64	3.344	26.51	3.360				(002)
	44.17	2.049	43.68	2.071				(110)
	52.24	1.750	52.80	1.733				(112)
CdS:Mn 4%	25.24	3.525	24.81	3.586	104	4.07	6.69	(100)
	26.64	3.344	26.51	3.360				(002)
	44.11	2.051	43.68	2.071				(110)
	52.24	1.750	52.80	1.733				(112)
CdS:Mn 6%	25.24	3.525	24.81	3.586	86	4.07	6.69	(100)
	26.64	3.344	26.51	3.360				(002)
	44.11	2.051	43.68	2.071				(110)
	52.24	1.750	52.80	1.733				(112)

The crystallite size (D) of the films grown on ITO substrates at different Mn dopant ratios was calculated from the diffraction peaks along (002) plane using the Scherer's formula:

$$D = \frac{0.9\lambda}{\beta cos\theta} \tag{1}$$

where θ and β are the Bragg's diffraction angel and the experimental full width at the half maximum (FWHM) in radians along (002) plane. The results indicated that the crystallite size decreased from 138 nm to 86 nm by increasing the Mn dopant, listed in Table 1.

Lattice constants a and c for the hexagonal structure were calculated using Eq. (2) and the results are also shown in Table 1.

$$\frac{1}{d_{hkl}^2} = \frac{4}{3}\left(\frac{h^2 + hk + k^2}{a^2}\right) + \frac{l^2}{c^2} \tag{2}$$

where d_{hkl} is the interplanar spacing of the crystallographic planes. The lattice constants are calculated as a = b = Σ4. 07 Å and c = 6.69 Å, shown in Table 1. As can be seen, these values are very close to the standard values ($a = b$ = 4.14 Å; c = 6.72 Å).

3.2. Morphological properties of CdS:Mn thin films

Three dimensional AFM images of the present films were shown in Fig. 3. It was seen that the surface morphology of the CdS thin film depends on Mn concentration. It was observed an increment in the number of spherical nanoparticles with different size and shapes on the film surfaces depending on an increment in the concentration of Mn. This means that crystallite size decreased from 138 nm to 86 nm with Mn. The roughness of the surface decreased with incorporation of Mn in the CdS films. These results indicated that both nanoparticle size and surface morphology are significantly affected by doping Mn.

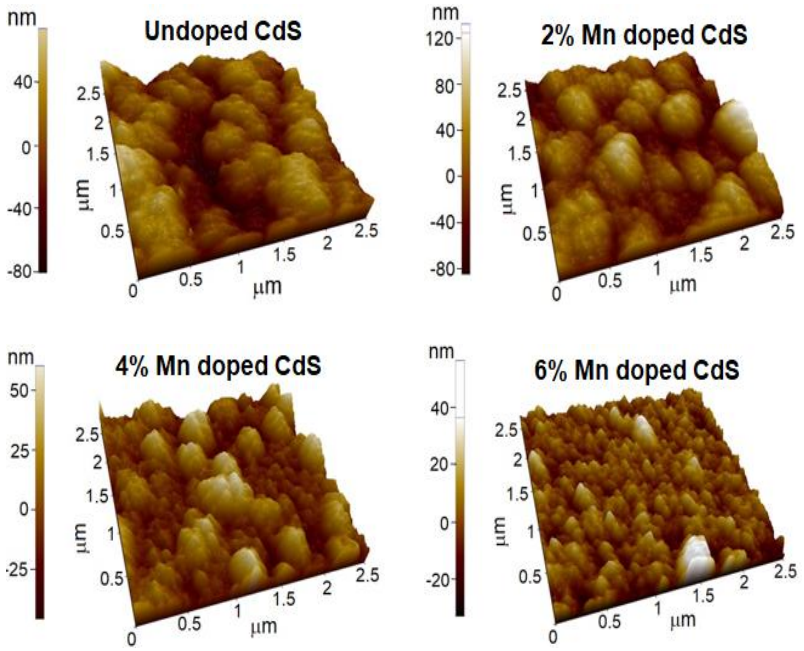

Fig. 3. Three dimensional AFM images of the CdS:Mn thin films.

3.3. UV-vis properties of CdS:Mn thin films

The optical absorption and transmittance spectra of the films were shown in Fig. 4(a) and (b), respectively. At wavelength of 480 nm, it was seen that the absorbance value of CdS thin film was 3% and it reduced to 2% with an increase in Mn concentration. In addition, transmittance value of the film varied between 41% and 73% in the visible range. The optical absorption of the CdS:Mn thin films were analyzed by the theory of band to band optical transition. The absorption coefficient (α) of the CdS:Mn thin films were calculated from the transmittance spectra using Beer-Lambert approximation using relation [18]:

$$\alpha = \frac{1}{d} ln\left(\frac{1}{T}\right) \tag{3}$$

where d is film thickness and T is transmission of the film. Film thicknesses of the investigated films were calculated from the interface patterns around 400–800 nm wavelengths using the Eq. (4):

$$d = \left\{2\left[\frac{n(\lambda_1)}{\lambda_1} - \frac{n(\lambda_2)}{\lambda_2}\right]\right\}^{-1} \tag{4}$$

where λ_1, λ_2 are adjacent maxima or minima and n is the refraction index (2.53) of the film. Calculated thickness values of the films were listed in Table 2. As seen, film thickness of pure CdS was 1764 nm first it decreased to the value of 774 nm and then increased to the value of 1624 nm again.

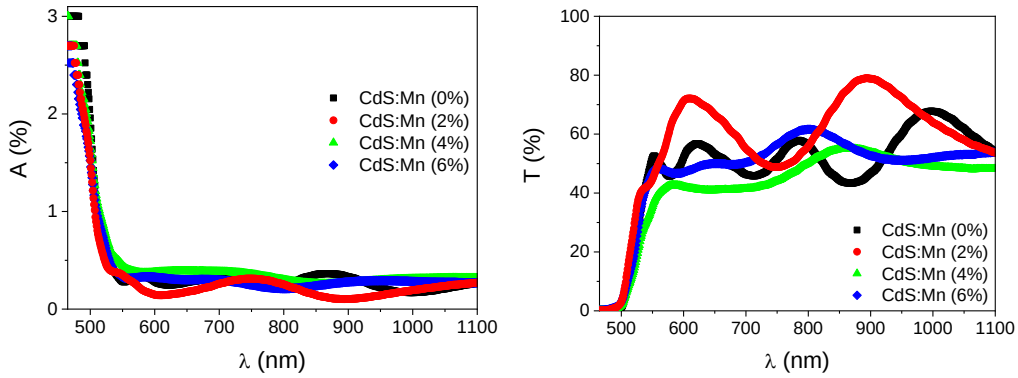

Fig. 4. Absorption and transmission spectra of the CdS:Mn thin films.

The optical band gap (E_g) of the films was determined by using theTauc's relation [18]:

$$\alpha h\nu = A\left(h\nu - E_g\right)^n \tag{5}$$

where $h\nu$ is the photon energy, A is a constant and n = 1/2 for direct allowed transition and n = 2 for indirect allowed transition. In order to determine whether the films had direct or indirect transition E_g $(\alpha h\nu)^2$ vs. ($h\nu$) and $(\alpha h\nu)^{1/2}$ vs. ($h\nu$) plots were drawn. Since better linearity was obtained in the $(\alpha h\nu)^2$ vs. ($h\nu$) plot in Fig. 5, the direct band gap values were estimated by extrapolating the linear portion of these plots to the energy axis. The E_g values of the films were presented in Table 2. It was seen that the E_g value of pure CdS thin film decreased from 2.43 eV to 2.41 eV with increasing Mn dopant. Moreover, in previous work [19], copper (Cu) incorporation into CdS thin film did not change optical band gap and it was determined as 2.42 eV for all deposited films. Using different methods, a reduction in band gap width with increasing different type of doping observed in different semiconductor thin films in literature [20-23]. A reduction in optical band gap width can be attributed to different factors such as carrier impurity interaction, carrier-phonon interaction, structural disorder [24] and defect states [25,26] in the CdS thin films with an increment in doping concentration of Mn.

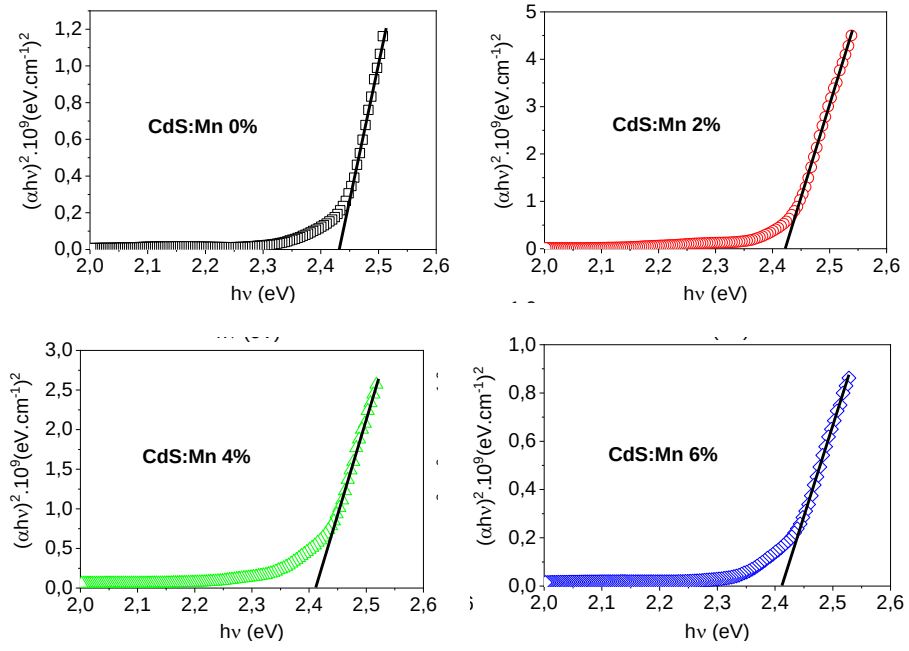

Fig. 5. Plot of $(\alpha h\nu)^2$ vs. $(h\nu)$ for the CdS:Mn thin films with different Mn dopant.

Table 2. Film thickness, band gaps and photoelectrical properties of DSSCs.

DSCCs	**Thickness (nm)**	E_g **(eV)**	V_{oc} **(V)**	J_{sc} **(mA cm^{-2})**	**FF (%)**	**η (%)**
CdS:Mn (% 0)	1764	2.43	1	8.46	40.14	**3.40**
CdS:Mn (% 2)	774	2.42	0.94	8.52	41.77	3.35
CdS:Mn (% 4)	1016	2.41	0.98	10.50	24.18	2.49
CdS:Mn (% 6)	1624	2.41	1	5.58	40.86	2.28

3.4. Dye-sensitized solar cell studies

The current-voltage (I–V) characteristics of hetero-junction (ITO/CdS:Mn/Murexid) DSSCs devices were gauged under bulb light of 7W white led lamp (after 1 h). The current density voltage (I–V) characteristics of DSSCs provide the information about the performance parameters of the cell such as short-circuit current density (J_{SC}), open-circuit voltage (V_{oc}), fill factor (FF) and energy conversion efficiency (η). The η was calculated using the following formula:

$$\eta = FF\frac{V_{oc}J_{sc}}{P_{in}} \tag{6}$$

where P_{in} is the intensity of the incident light (W / cm^2) of the DSSC and FF is determined using the following equation:

$$FF = \frac{V_m I_m}{V_{oc}J_{sc}} \tag{7}$$

where $V_m I_m$ is the maximum power output of the cell per unit area. The J-V characteristic of the DSSCs gauged under bulb light of 7W led lamp were given in Fig. 6. In addition, determined cell parameters were listed in Table 2. The DSSCs fabricated utilizing pure CdS thin film, which were lightened using 7W white led lamp, showed maximum performances with an efficiency (η) of 3.40%, an open-circuit voltage (V_{oc}) of 1 V, a fill factor (FF) of 40.14%, and a short-circuit current density (J_{sc}) of 8.46 mA.cm^{-2}. It was clearly seen that conversion efficiency decreased from 3.40% to 2.28% with an increase in Mn concentration after lightening. This indicated that introducing Mn dopant into CdS film did not make a favourable effect on performance of the DSSC. Our conversion efficiency values were higher than the values in the literature [27–34]. Moreover, present efficiency values were consistent with the earlier results [16,35–37].

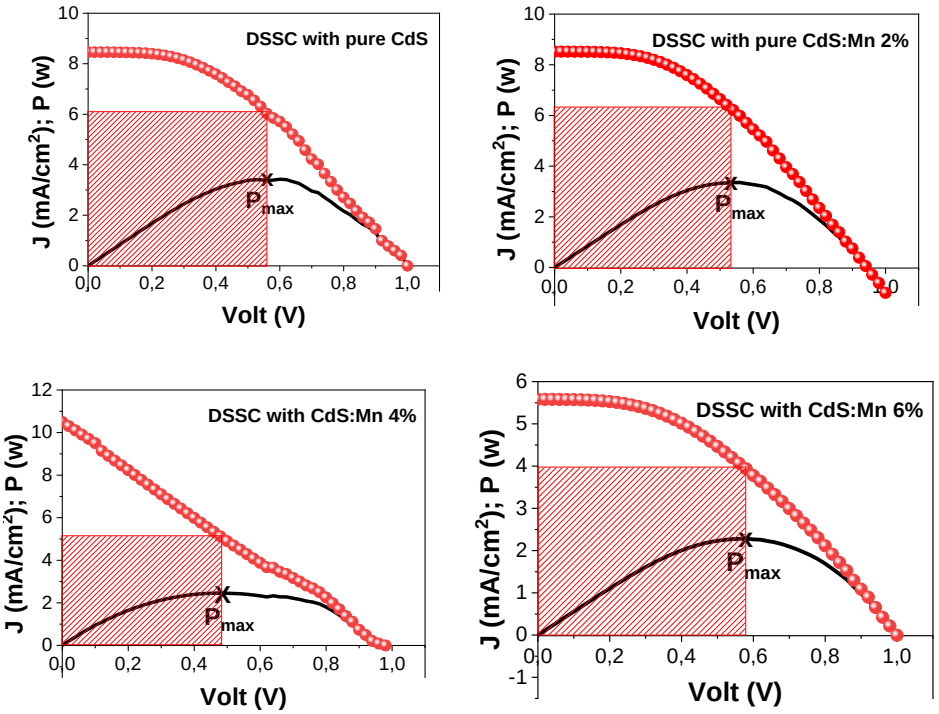

Fig. 6. J-V characteristic of ITO/CdS:Mn/Murexid DSSCs.

4. Conclusions

In summary, the DSSCs (ITO/CdS:Mn/Murexid) were designed using Murexid dye and inorganic CdS:Mn thin films onto ITO substrates via chemical bath deposition which is a low cost technique. In this work, we used Murexid dye and the CdS:Mn thin films for designing the DSSCs for the first time. The XRD analysis indicated that all deposited CdS:Mn thin films had polycrystalline with hexagonal structure. The results obtained from XRD and AFM analyses showed that both crystallite size and nanoparticle size decreased with increasing Mn doping concentration. Optical band gap value was decreased from 2.43 eV to 2.41 eV by doping Mn. Our experimental results indicated that incorparation of Mn into CdS film for the fabrication of DSSCs did not make any favorable effect on performance of the device, but we achieved the highest photoelectric conversion efficiency of 3.40% for the DSSC designed using pure CdS thin film (ITO/CdS/Murexid).

Based on the above results, it can be concluded that we have improved solar energy efficiency of DSSCs which is fabricated using Murexid dye and inorganic CdS:Mn thin films. In addition, we consider that the high-cost of DSSCs can be reduced by using a cheap dye and CBD method that is simple and economical. Furthermore, this work is also important in that it involves the use of a waste product. We hope that DSSCs can be a good alternative to silicon-based cells which cost much.

Acknowledgements

This study was partially supported by Burdur Mehmet Akif Ersoy University, Burdur, Turkey under Project Grant no. 0348-NAP-16.

References

[1] F. Göde, S. Ünlü, Mater. Sci. Semicond. Process. **90**, 92 (2019).
[2] S. A. Taya, T. M. El-Agez, M. S. Abdel-Latif, H.S. El-Ghamri, A. Y. Batniji, I. R. El-Sheikh, Int. J. Renew. Energy Res. **4**(2), 384 (2014).
[3] G. Calogero, G. Di Marco, Sol. Ener. Mater. Sol. Cells **92**, 1341 (2008).
[4] E. Yamazaki, M. Murayama, N. Nishikawa, N. Hashimoto, M. Shoyama, O. Kurita, Solar Energy **81**, 512 (2007).
[5] V. Shanmugama, S. Manoharan, S. Anandan, R. Murugan, Spectrochim Acta A. **104**, 35 (2013).
[6] M. F. Abdelbar, T. A. Fayed, T. M. Meaz, T. Subramani, N. Fukata, El-Z.M. Ebeid, J. Photochem. Photobiol. A Chem. **375**, 166 (2019).
[7] H. Gerischer, M.E. Michel-Beyerle, F. Rebentrost, H. Tributsch, Electrochim. Acta. **13**, 1509 (1968).
[8] H. Tsubomura, M. Matsumura, Y. Nomura, T. Amamiya, Nature **261**, 402 (1976).
[9] Y. Chiba, A. Islam, Y. Watanabe, R. Komiya, N. Koide, L. Han, Japanese J. Appl. Phys. **45**(25), L638 (2006).
[10] R. Buscaino, C. Baiocchi, C. Barolo, C. Medana, M. Grätzel, Md. K. Nazeeruddin, G. Viscardi, Inorg. Chim. Acta. **361**(3), 798 (2008).
[11] B. O'Regan, M. Graetzel, Nature **353**, 737 (1991).
[12] M. I. Khan, M. Saleem, S. Ur Rehman, R. Qindeel, M. S. Ul Hassan, I. Ahmad, H.S. J. Nanoelectron. Optoelectron. **13**(7), 1090 (2018).
[13] J. B. Baxter, A. M. Walker, K.Van Ommering, E. S. Aydil, Nanotechnology **17**(11), S304 (2006).
[14] R. Bhattacharjee, I.-M. Hung, Mater. Chem. Phys. **143**(2), 693 (2014).
[15] K. R. Aneesiya, C. Louis, J. Alloys Compd. **829**, 154497 (2020).
[16] I. Y. Y. Bu, Optik **205**, 164242 (2020).
[17] A. K. Rajan, L. Cindrella, Superlattices Microstruct. **128**, 14 (2019).
[18] J. Tauc, Amorphous and Liquid Semiconductors, Springer Science & Business Media, New York, 2012.
[19] F. Göde, Optik **197**, 163217 (2019).
[20] A. K. Ambedkar, M. Singh, V. Kumar, V. Kumar, B. P. Singh, A. Kumar, Y. K. Gautam, Surf. Interfaces **19**, 100504 (2020).
[21] I. B. Jemaa, F. Chaabouni, A. Ranguis, J. Alloys Compd. **825**, 153988 (2020).
[22] S. Moghe, A. Acharya, R. Panda, S.B. Shrivastava, M. Gangrade, T. Shripathi, V. Ganesan, Renewable Energy **46**, 43 (2012).
[23] I. S. Yahia, I. M. El Radaf, A. M. Salem, G. B. Sakr, J. Alloys Compd. **776**, 1056 (2019).
[24] N. F. Mott, E. A. Davis, Electronic Process in Non-Crystalline Materials, Calendron Press, Oxford, 1979.
[25] S. Rajendran, M. M. Khan, F. Gracia, J. Qin, V.K. Gupta, S. Arumainathan, Sci. Rep. **6**, 1 (2016).
[26] K. Vijaylakshmi, D. Sivaraj, RSC Adv. **5**(84), 68461 (2015).
[27] F. A. Unal, S. Ok, M. Unal, S. Topal, K. Cellat, F. Şen, J. Mol. Liq. **299**, 112177 (2020).
[28] P. Gu, D. Yang, X. Zhu, H. Sun, J. Li, Chem. Phys. Lett. **693**, 16 (2018).
[29] N. Mir, M. Salavati-Niasari, F. Davar, Chem. Eng. J. **181–182**, 779 (2012).
[30] N. E. Safie, N. A. ludin, N. H. Hamid, S. Sepeai, M. A. M. Teridi, M. A. Ibrahim, K. Sopian, H. Arakawa, Mater. Renew. Sustain Energy **6**(2), 5 (2017).
[31] D. Gebeyehu, C. J. Brabec, N. S. Sariciftci, Thin Solid Films **403–404**, 271 (2002).
[32] D. J. Godibo, S. T. Anshebo, T. Y. Anshebo, J. Braz. Chem. Soc. **26**(1), 92 (2015).
[33] R. Ramanarayanan, P. Nijisha, C. V. Niveditha, S. Sindhu, Mater. Res. Bull. **90**, 156 (2017).
[34] C.-C. Yuan, S.-M. Wang, W.-L. Chen, L. Liu, Z.-M. Zhang, Y. Lu, Z.-M. Su, S.-W. Zhang, E.-B. Wang, Inorg. Chem. Commun. **46**, 89 (2014).
[35] B. Pang, Y. Shi, S. Lin, Y. Chen, J. Feng, H. Dong, H. Yang, Z. Zhao, L. Yu, L. Dong, Mater. Res. Bull. **117**, 78 (2019).
[36] R. Sivakumar, K. Akila, S. Anandan, Curr. Appl. Phys. **10**, 1255 (2010).
[37] A. G. Al-Sehemi, A. Irfan, M. A. M. Al-Melfi, Spectrochim. Acta A **145,** 40 (2015).